

SMOV: COS FUV Focus Determination

Daniel Lennon¹, Cristina Oliveira¹, George Hartig¹, Eric Burgh², Cynthia Froning²,
Steve Osterman², Sami Niemi¹, Graham Harper², Parviz Ghavamian¹,
Charles D. Keyes¹

¹ Space Telescope Science Institute, Baltimore, MD

² Center for Astrophysics and Space Astronomy, University of Colorado, CO

04 March 2010

ABSTRACT

The procedures for determining the COS FUV fine-focus for the G130M, G160M and G140L gratings are described and it is shown that auto-correlation, simulation and fourier transform methods of analyzing the focus-sweep data provide consistent and robust estimates of the focus off-sets required to reach optimal focus position for the G130M and G160M gratings of COS.

Contents

- Introduction (page 2)
- Initial Focus Determination (page 2)
- Final Focus Determination (page 5)
- Final Considerations (page 10)
- Change History (page 11)
- References (page 11)
- Appendices (page 11)

1. Introduction

This report describes the analysis and conclusions relating to the determination of COS FUV fine-focus positions for the G130M, G160M and G140L gratings during SMOV. The original data for this purpose were obtained as part of the program described under SMOV activity COS26, with proposal number 11484, entitled ‘FUV Optics Alignment and Focus’ (P.I. Keyes), visits 01, 02 and 03 performing the initial focus sweeps with visits 05 and 06 being used for confirmation. A subsidiary goal of this activity was to perform initial tests of the dispersed light target acquisition performance which is not discussed in this report. During SMOV a first analysis of the data revealed that the spectra obtained in the original program were inadequate for estimating a reliable focus, in particular for the G130M and G160M gratings. Additional visits, and a new target, were therefore added to proposal 11484 to improve the focus determination for these two gratings. In the report we first summarize the original program, its results and their deficiencies (Section 2), and then go on to describe the revised activity and its results (Section 3), finishing with some comments and observations (Section 4).

2. Initial Focus Determination

The basic procedure employed to determine the fine-focus is to take a series of spectra of an astronomical source for a range of focus off-sets which scan through the expected focus position, this position having been determined in ground testing. The best focus position is then determined by fitting the full-width half maximum (FWHM) of lines (emission or absorption) as a function of focus position and determining the minimum of this function (typically a quadratic/parabolic function). As COS is effectively a slit-less spectrograph with performance optimized for a well centered source in the entrance aperture one requires the target to be a point source with strong and narrow absorption or emission lines unresolved by the instrument. The goal is to determine the best focus to within 50 steps of the Optical Select Mechanism 1 (OSM1) so the step increments are set at 100 steps. Since the actual telescope focus is subject to breathing excursions comparable to this step-size the focus offsets are corrected for breathing using the OTA breathing model.

The initial focus sweep used an O-type star IDH52-2 of spectral type O2 lying in the Large Magellanic Cloud (LMC) as the target for the G130M and G160M gratings (visits 01 and 02), while the QSO H-1821+643 was used for the G140L focus sweep (visit 03). The widths of strong Interstellar Medium (ISM) or Intergalactic Medium (IGM) lines were measured and used to construct the focus sweep diagrams shown in Fig.1. Note that Fig.1 does not show results for the G160M grating as these data were found to have lower signal-to-noise than expected¹ and a reliable measurement of ISM line widths was not possible. As can be seen from Fig.1 the G130M focus sweep

¹Probably due to the application of an inappropriate extinction law. We note that the FUV fluxes for IDH52-2 were estimated using the Milky Way extinction law as it was known that the standard LMC extinction law gave higher than typical UV extinction due to its bias towards 30 Doradus stars with their higher than usual FUV extinction. However IDH52-2 lies in the vicinity of 30 Doradus and its extinction

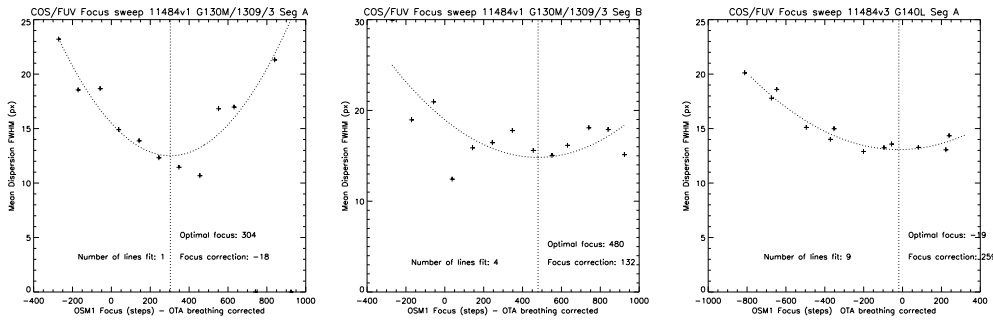


Figure 1. Each of the above trends compares the mean FWHM of absorption lines as a function of OTA breathing corrected focus position, where this position is given as the OSM1 absolute position (in steps). The two panels on the left illustrate the focus sweep results for the G130M grating on segments A and B of the FUV detector, while the rightmost panel is the result for the G140L grating on segment A. The dashed lines are parabolic fits to the points, and the vertical dashed lines indicate the position of the minima, or optimal focus positions. The G140L segment B spectrum did not contain suitable absorption lines for this procedure.

suffered somewhat from the same problems; it was only possible to use a single line in the Segment A data, while the Segment B data did not exhibit a strong minimum. The G140L data on the other hand were rather better, 9 lines were measured with some degree of confidence, albeit the minimum was a little close to the edge of the focus sweep. Based on these results it was decided to move all three FUV gratings by the same amount of +150 steps, based mostly on considering the G140L data and assuming that the relative focus positions should not differ from those determined during ground testing. Following the focus move a confirmation spectrum was obtained in subsequent visits (05 and 06) to the same targets.

Following the focus move there were a number science observations related to the ERO program and some concerns were raised that COS in fact was not at optimum focus. Accordingly the focus sweep data were carefully re-examined to investigate this suggestion further. As it had been found that the FWHM of the ISM lines in IDH52-2 were not sensitive diagnostics of the focus position we concentrated on visual inspection of the detail in the cores of these lines. Such lines should in principle have multiple components although note that there have been no previous UV observations of IDH52-2. Fig.2 shows an example of the focus sweep spectra at the position of the Si I multiplet (number 23) which indicates that the nominal² focus position is most likely closer to the best focus position than the new position (at an offset of +150 steps). Of course these spectra have been interpreted without referring to the breathing focus corrections but these are typically less than the equivalent of 100 steps. Furthermore, we repeated this

is most probably well represented by the standard LMC law.

²Here we use 'nominal focus' to refer to the initial best focus positions or zero-points as determined during ground testing.

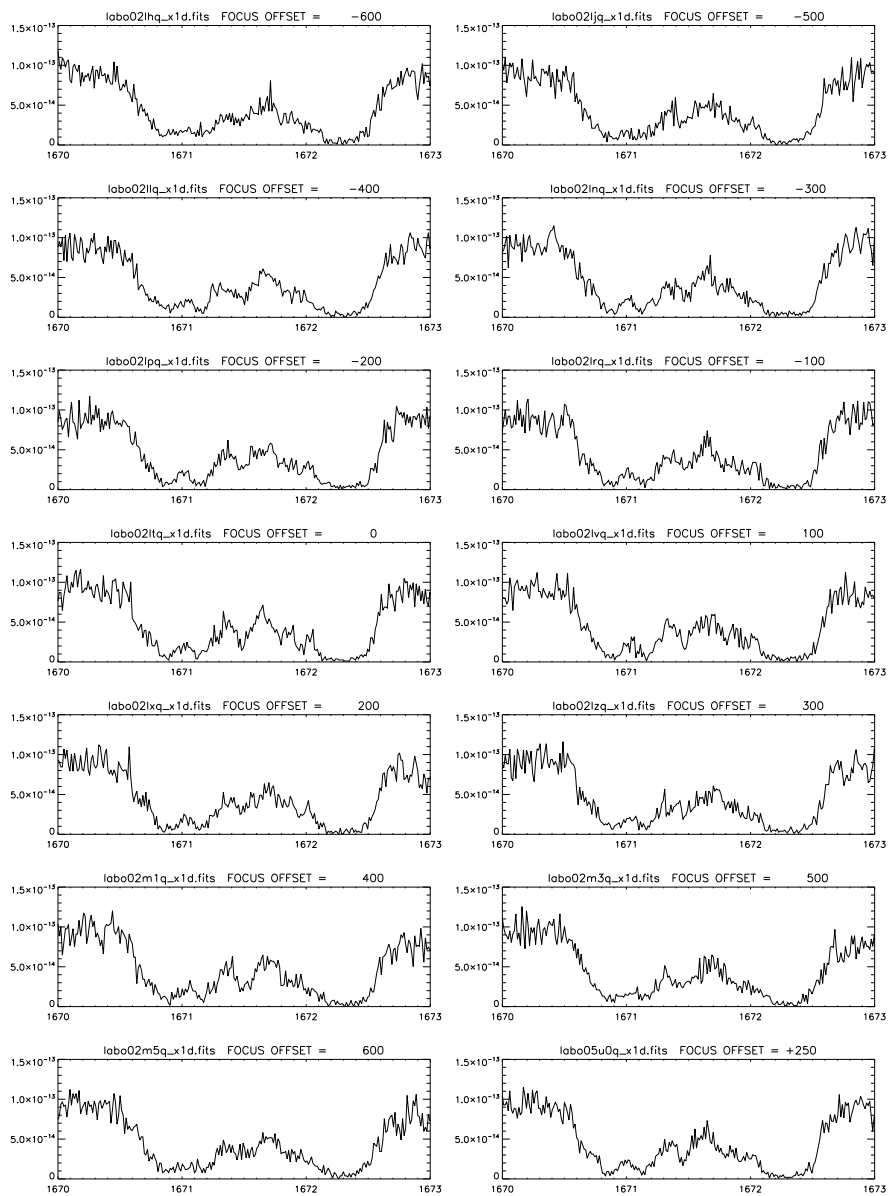


Figure 2. This series of panels shows the observed Si I multiplet for the G160M grating focus sweep. The spectra are ordered left to right and then top to bottom in order of increasing focus position. The nominal focus position is therefore the fourth panel down on the left. There are 13 observations in the focus sweep, separated by 100 steps of OSM1, beginning at an offset of -700. The fourteenth panel on the bottom right was taken after the focus move. All exposure times were identical. Careful inspection of the degree of detail apparent in the line profile cores shows that the best focus is given by the spectrum taken at the nominal focus position while that at +100 steps is better than the spectrum at -100 steps. The confirmation spectrum, bottom right, is clearly not as good as that taken at the previous nominal position.

detailed inspection for other ISM lines in IDH52-2 for both the G130M and G160M gratings and both segments and concluded that we moved away from the best focus position which is in fact closer to the nominal for both gratings. In the following section we describe the corrective actions which were undertaken to determine new focus positions.

3. Final Focus Determination

The realization that the ISM lines in IDH52-2 were inadequate for the purpose of quantifying the best focus position led to a reassessment of suitable targets. Ideally we required a point source with narrow lines, unresolved at the nominal resolution of COS (15 km/s), and faint enough to pose no danger to the detectors. We opted for Feige 48 (with aliases KL UMa, PG1144+615) which is an sdB star with a very low projected rotational velocity (< 5 km/s) and very many metal absorption lines in the UV. While Feige 48 is also a single lined spectroscopic binary its period is 9.6 hours and velocity amplitude is 28 km/s (O'Toole et al. 2004), hence the velocity smearing during single exposures (of length 96, 180 and 400 seconds) is negligible for our purposes. Furthermore, there are excellent STIS/E140M data for this star allowing us to estimate what we should observe with COS.

One concern with this target was that the density, and blending, of stellar absorption lines might make it difficult to determine a good focus position due to the difficulty of finding isolated strong lines. We therefore adopted two independent methods which should be robust and make use of the many hundreds on lines in the spectrum. We discuss each of these methods in turn, and in addition we mention two additional methods which were subsequently added as further independent corroboration.

- **Auto-correlation:** This method relies on the fact that the width of the auto-correlation function is determined by the widths of the lines in the spectrum, broader lines lead to a broader auto-correlation function. Of course not all lines in a spectrum have the same width, however in the case of Feige 48 the spectrum is dominated by many hundreds of metal lines whose intrinsic widths are essentially determined by the projected rotational velocity (< 5 km/s) and are effectively unresolved by COS. Hence their widths are determined by the resolution of the instrument which in turns depends on the focus. We make use of the power in these lines, and can mitigate against the effects of very strong lines which might be either inter-stellar lines or strongly pressure broadened stellar lines, by selecting regions of each spectrum with care. One advantage of this method is that it is empirical and does not rely upon knowledge of the resolution.
- **Simulation:** This method's philosophy is similar to the above but differs in that we compute a series of spectra by convolving a gaussian kernel of various FWHM_a with the template STIS E140M spectrum. The best matching FWHM for each observed spectrum is then obtained (chi-squared test) enabling us to construct the focus curve.

Table 1. Focus off-set results of auto-correlation analysis for each quadrant of segments A and B for the G130M and G160M gratings. Taking straight means of these values for the G130M and G160M gratings gives focus off-sets of -286 and -205 steps respectively, where we exclude the out-lying value of -49 (G130M, Segment B, Quadrant 3) from this computation.

Grating	Segment	Quadrant 1	Quadrant 2	Quadrant 3	Quadrant 4
G160M	B	-239	-188	-213	-208
G160M	A	-289	-130	-229	-149
G130M	B	-247	-351	-49	-188
G130M	A	-224	-383	-304	-313

- **Fourier Transform:** This is essentially similar to the auto-correlation method except that it works in the Fourier domain.
- **Visual check:** As this implies, all the focus run data should be visually inspected to check that the best focus position is indeed being found by these approaches.

Before applying this to the real data it was decided to carry out a blind test of these methods (excluding the FT method) in order to check that the methods work, and as practice to ensure fast turn-around of the analysis. This blind test consisted of the IDT simulating a focus run of Feige 48 using the optical model of COS and model line spread function (LSF) such that the true best focus position was unknown to the analysis team. Three simulations were performed, one for each of the G130M and G160M gratings, plus an additional simulation for the G160M grating including interstellar lines to assess the impact of these on the result. The team had then to derive the focus position from these data, which was then compared with true position. The results of this exercise were extremely successful, finding the correct focus position to within 50 steps as required.

The COS FUV focus runs were therefore repeated with Feige 48, albeit with one difference in that the G130M exposure was split into separate Segment A and B observations to avoid exceeding global count rate limits (visits 93, 94 and 95). The 13 individual exposures were centered at the previous nominal value of the focus position, i.e. identical to that used for IDH52-2. There are thus three sets of focus run data using Feige 48; G130M Segment A, G130M Segment B, and G160M (Segments A and B taken simultaneously). The relevance of this is that each of the G130M datasets has different breathing corrections which results in a total of 26 unique focus positions when combining Segment A and B data. (We assume that both segments have the same focus position which is justified from consideration of ground test data.)

In applying the auto-correlation method to the data we split each segment into quadrants, avoiding strong inter-stellar lines if possible, and processed each of these

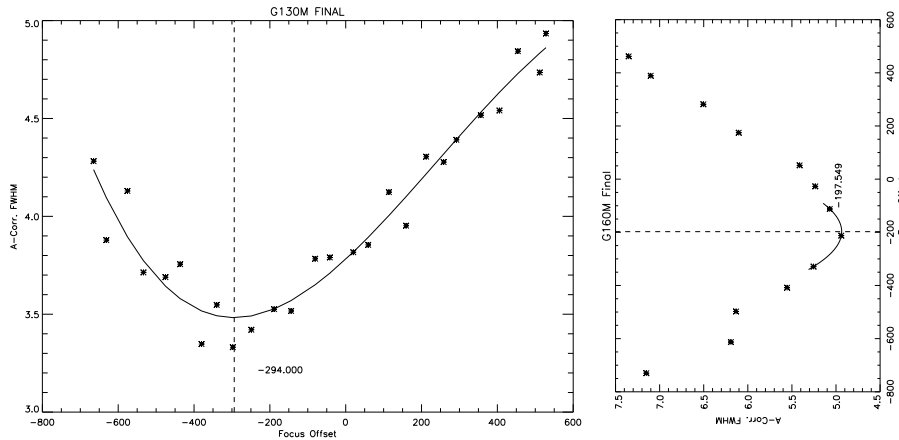


Figure 3. The final result of the G130M and G160M focus sweeps are in the left and right hand panels respectively where FWHM of the auto-correlation functions are plotted as a function of focus off-set. Since the Segment A and B observations for the G130M grating were taken at different times the breathing corrections were different resulting in two separate data-sets. These points were fit with a single cubic function in order to derive the minimum and best focus position. The G160M Segment A and B observations were taken simultaneously and the various measurements were therefore combined into this single mean set of points and the minimum derived using a simple quadratic interpolation about the minimum point.

quadrants separately. This resulted in eight focus curves per grating, four for each segment, from which the minima were estimated using quadratic interpolation around the minimum point, as shown in Table 1. Taking means of these values gives off-sets of -286 steps for the G130M grating and -205 steps for the G160M grating, where we exclude one outlying value as described in Table 1. One can also construct final focus curves for the G160M by simply taking the mean of the FWHM values at each focus position, while for the G130M grating one does this for each segment (note the different breathing corrections) before merging the points onto a single focus curve. The results are shown in Figure 3 from which one can see that the focus off-set positions are determined to be -294 and -198 steps for the G130M and G160M gratings respectively, which are in very good agreement with straight mean values discussed above.

In the simulation approach each spectrum is first broken into 10–20 Ångström chunks, each of which is used to determine a best-matching FWHM, from which a mean value was determined at that focus position. The results of this procedure are illustrated in Figure 4, note that breathing corrections have not been applied to the individual focus positions. Fortunately during each focus run the breathing corrections varied little and so we applied mean breathing corrections of +105 steps to the G130M Segment B values, +60 steps to the G130M Segment A values, and +37 steps to the G160M values (both segments). Putting these together with the results from Figure 4 gives us focus off-sets of -289 and -190 steps for the G130M and G160M gratings

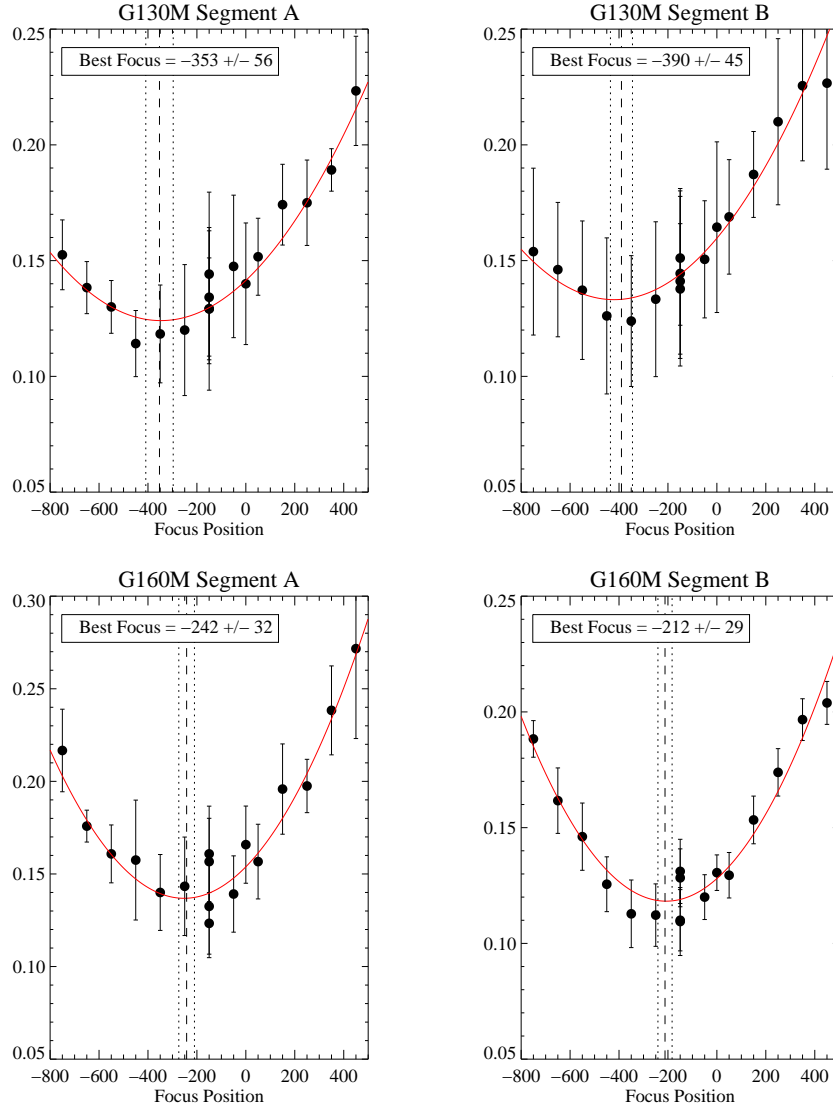


Figure 4. The results of the G130M and G160M focus sweeps using the simulation method, the y-axis in each panel is a measure of the FWHM of the gaussian kernel representing the best fit to the spectrum when convolved with the template STIS E140M spectrum of Feige 48. Note that the focus positions in these plots are not breathing corrected.

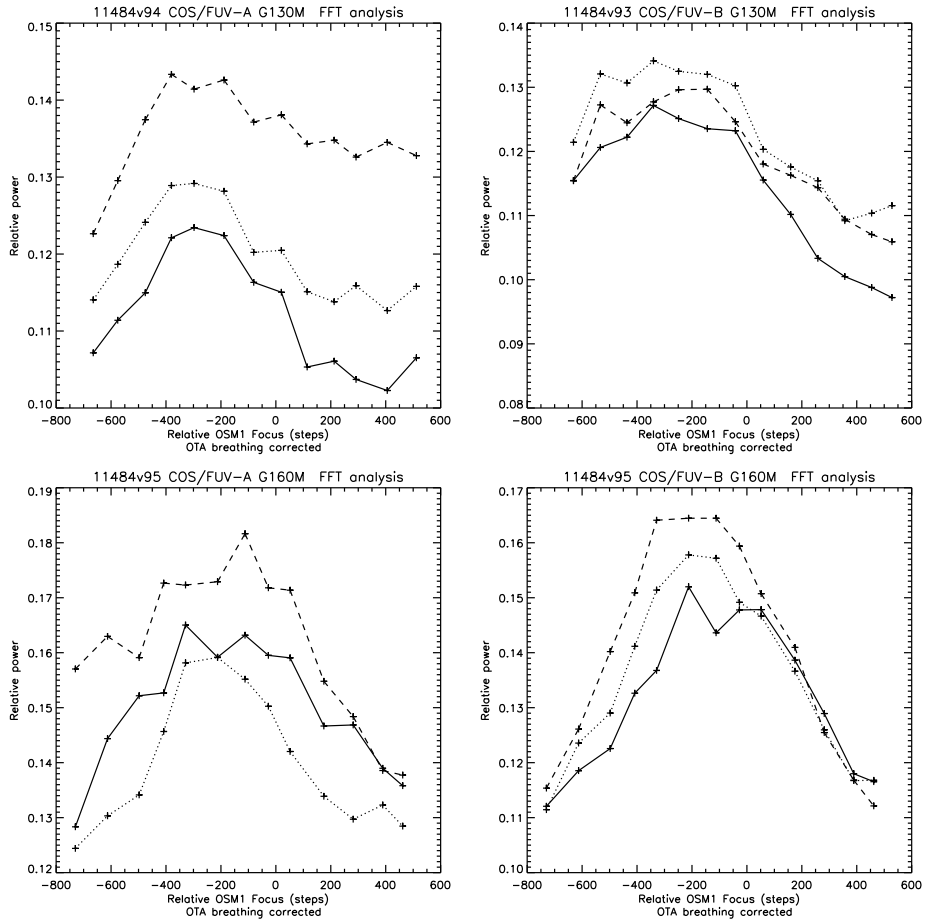


Figure 5. The focus results from the Fourier transform analysis. Each of the three curves per panel are solutions for separate regions of the spectrum in each segment.

Table 2. Final focus off-set results of auto-correlation, simulation and fourier transform analyses for the G130M and G160M gratings. Recommended values are in the second-last column. Note that these are relative to the revised focus positions from section 2 which are at +250 steps relative to the launch nominal positions. We also include the revised focus position for the G140L grating as discussed in the text.

Grating	Auto-correlation	Simulation	Fourier Transform	Recommended	Relative to nominal
G130M	-294	-289	-300	-300	-50
G160M	-198	-190	-200	-200	+50
G140L	-	-	-	+100	+250

respectively. Similar results are found from the Fourier transform approach (Figure 5) where we estimate focus off-sets of -300 and -200 steps, and a visual inspection of the data was consistent with these results. Table 2 summarizes these findings.

We also note here that while the G140L focus was not repeated the original focus data were re-assessed since the initial focus move was to some extent a compromise between all three grating results. From Fig.1 it is clear that the quality of the solution for the best focus position is quite reasonable, with a predicted offset of +250 steps. We therefore decided to move the G140L focus position by a further +100 steps, as indicated in Table 2.

4. Final Considerations

It should be noted that this work was carried out before we became fully aware of the issue with the COS LSF (Ghavamian et al 2009) and it was assumed that the LSF was well approximated by a gaussian function. In retrospect this perhaps contributed to the difficulty in using the saturated interstellar lines in IDH52-2 to determine the focus since their cores were filled in by the extended wings of the LSF. It would be interesting to repeat the simulations discussed above using a more appropriate LSF to see how this might change the focus determination, although given the excellent agreement between all methods it seems unlikely that any such correction would be significant. The auto-correlation method in particular seems robust and works independently of any knowledge of the LSF, though more careful choice of spectral regions might refine the results a little more. This method might also have some merit in providing some corroboration for the shape of the LSF. Finally, the G140L focus sweep data might be worth revisiting using methods similar to those described in section 3 to see if it is possible to confirm the best focus position using those techniques. As a final corollary to his exercise we note that the best focus positions of all three gratings have shifted relative to each other since launch suggesting that their focus should be monitored individually in subsequent calibration programs.

Table 3.

Filename sequence	Target name	Description
labo01020 – labo010e0 (13 files)	IDH52-2	G130M focus run, Segments A & B
labo02020 – labo020e0 (13 files)	IDH52-2	G160M focus run, Segments A & B
labo03010 – labo010d0 (13 files)	H-1821+643	G140L focus run, Segments A & B
labo93030 – labo930f0 (13 files)	Feige 48	G130M focus run, Segment A
labo94030 – labo940f0 (13 files)	Feige 48	G130M focus run, Segment B
labo95030 – labo950f0 (13 files)	Feige 48	G160M focus run, Segments A & B

5. Change History for COS ISR 2010-07

Version 1: 1 04 March 2010 - Original Document

6. References

Ghavamian, P. et al, 2009, COS Instrument Science Report 2009-01
O’Toole, S.J. et al. 2004, A&A, 422, 1053

Appendix A

Table 3 of this appendix lists the filenames of the data from program 11484 which were used in the analysis presented in this ISR.